# CHAPTER IV
# RESULT AND DISCUSSION

Chapter IV will discuss and analyze the experimental results from the testing magnetic field calculations with various cases, such as Reference measurement and Special cases. Moreover, using NV center allows unknown magnetic field mapping from ODMR signals.

## 4.1 Validation measurements

Prior to measurement, the setup is validated by observing all Zeeman-effect-induced splitting cases, ranging from one to four splittings in the ODMR signal. These splittings reflect the orientation of the applied magnetic field relative to the four crystallographic axes of the NV centers. When the magnetic field is oriented perpendicular to an NV axis, the ODMR spectrum exhibits a single splitting. This indicates that all four NV orientations experience the magnetic field with the same magnitude and direction.

In contrast, when the magnetic field is not perpendicular to the NV axes, the ODMR signal displays between two and four splitting. A four-splitting scenario implies that each NV axis senses the magnetic field with a distinct direction and magnitude. In the case of two or three splitting, this suggests that certain NV axes are exposed to identical magnetic field vectors, resulting in overlapping resonance frequencies. Thus, some splitting may represent multiple NV orientations.

To establish a reference dataset, measurements are conducted under controlled magnetic field orientations to produce each type of splitting. Specifically, a single splitting is achieved with $\theta$ = 90° and $\phi$ = 0°, two splitting with $\theta$ = 80° and $\phi$ = 0°, three splitting with $\theta$ = 80° and $\phi$ = −10°, and four splitting with $\theta$ = 70° and $\phi$ = −10°. These reference signals serve as benchmarks for later magnetic field analysis.

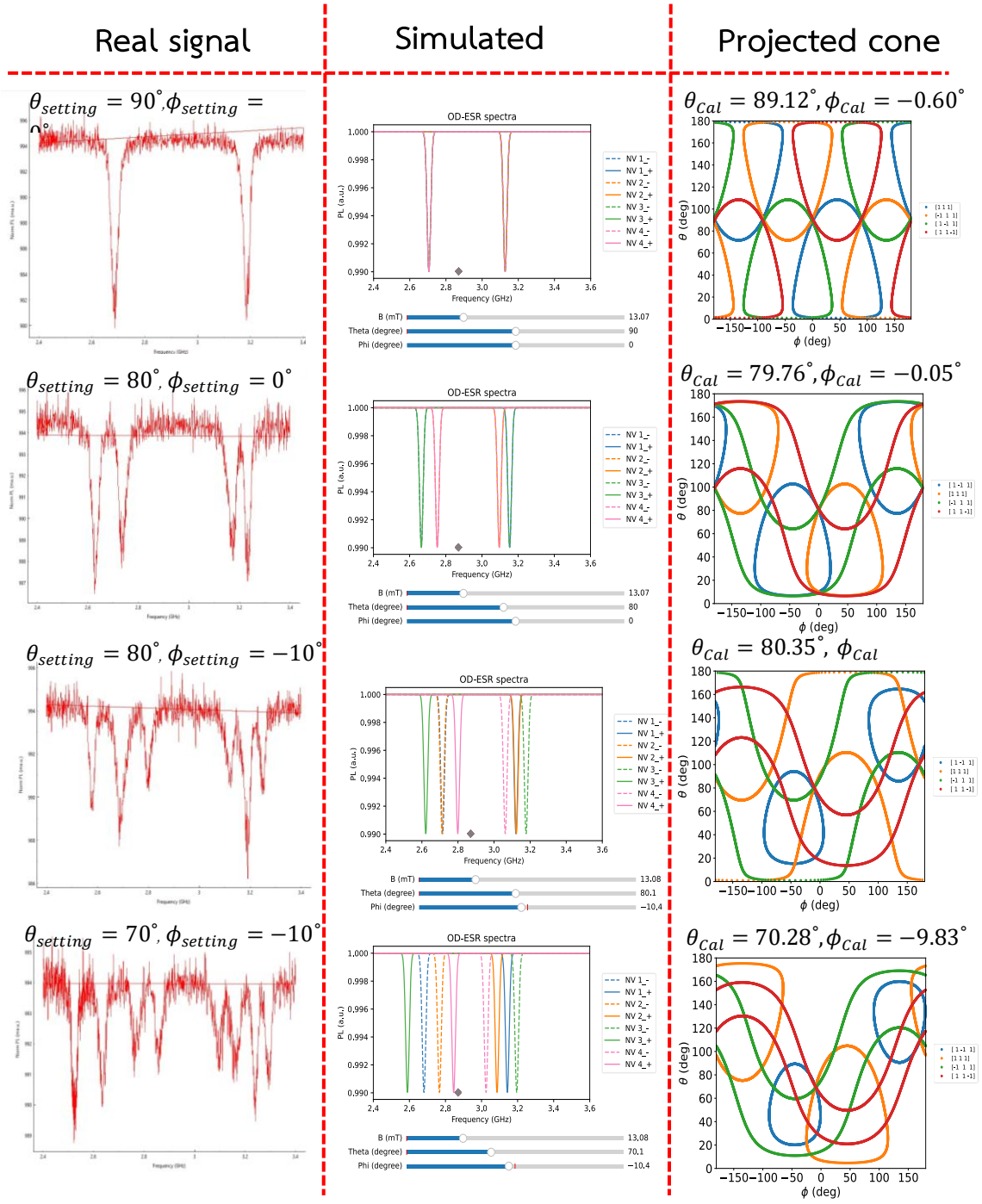


**Figure 4.1** Result from magnetic field calculation represents comparison between real signal, simulated signal and projected cone. The Real signal is the detected ODMR signal. The simulated signal from the simulation program is to match NV axes and ODMR splitting. The projected cone is the calculated results.

Magnetic field calculations are based on these reference data to determine both field magnitude and orientation. Accurate determination of the NV axes associated with each splitting is necessary and is achieved using a simulation program based on the Hamiltonian of the NV center. The program allows adjustment of the magnetic field strength ($B$), polar angle ($\theta$), and azimuthal angle ($\phi$) to produce a simulated ODMR spectrum that closely matches the measured reference data. This process ensures that the simulated signals reflect the actual NV axis orientations.

For consistency, each reference splitting case must correspond to the same calculated magnetic field magnitude. The resulting field magnitudes are closely aligned, with values of 153.05 G, 162.55 G, 157.10 G, and 167.84 G for one to four splitting cases, respectively. Magnetic field orientation is then determined from the reference data using the simulation-based calculation, and the resulting vector orientations are validated through graphical analysis of their intersections. This confirms the accuracy and reliability of the magnetic field method in Figure 4.1.

## 4.2 Resolution test

This topic proves that magnetic field calculations can distinguish similar ODMR signals of different magnetic field orientations, and ODMR signals from small angle changes.

### 4.2.1 Magnetic field from different directions with similar ODMR signal

In this case, although the magnetic field orientation angles differ, both configurations produce observable ODMR signals. The red ODMR signal corresponds to a magnetic field orientation of $\theta$ = 150° and $\phi$ = 50°, while the blue ODMR signal corresponds to $\theta$ = 160° and $\phi$ = 70°. The ODMR spectra exhibit similar overall profiles, with some splitting occurring at identical frequency positions. However, a notable difference is observed in the third splitting of the blue ODMR signal, which shifts closer to the second splitting of the red signal with black arrows in Figure 4.2.

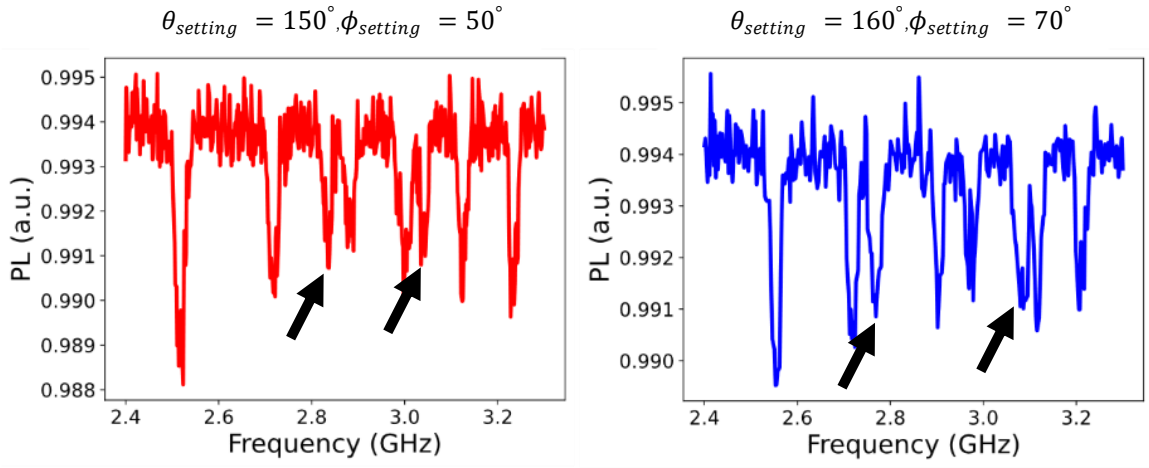


**Figure 4.2** Two ODMR signals with similar shape acquired when $\theta$ and $\phi$ is set to 150°, 50° (red), and 160°, 70° (blue). The third splitting of red ODMR is shift close to second splitting in the blue ODMR following the black arrow.

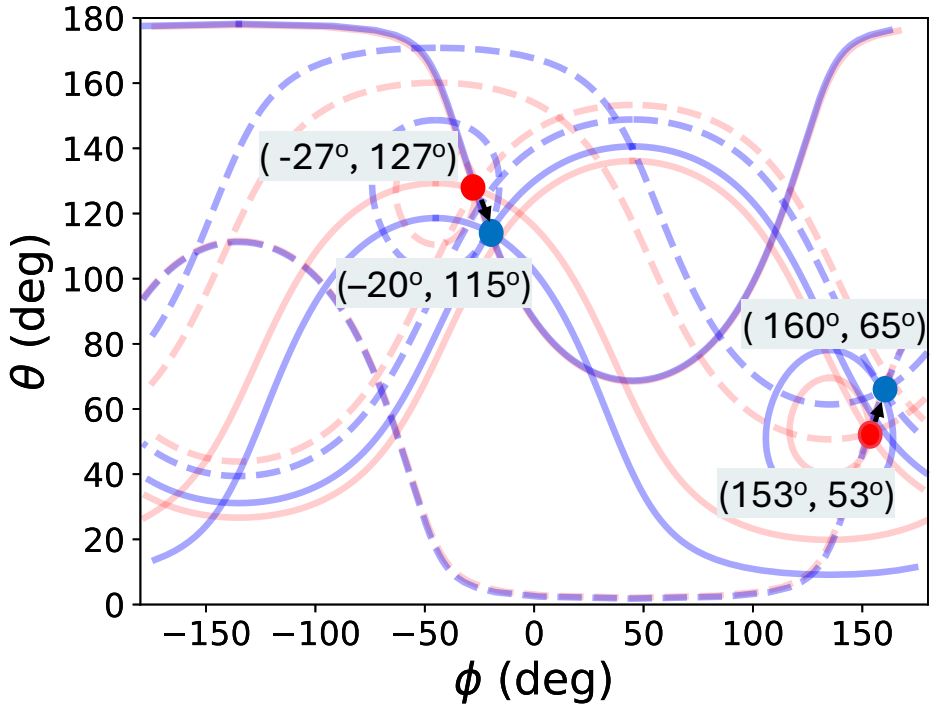


**Figure 4.3** the calculation result of the first special case. The blue and red curves are the calculated results of NV axes that sense magnetic field from the blue and red ODMR signal respectively. The interceptions of blue and red curves are orientation of magnetic field.

To analyze this phenomenon, magnetic field orientation is determined through computational reconstruction. The calculated results yield solution sets for both ODMR signals in spherical coordinates. In the corresponding graphical representation, the red and blue curves represent the solution sets for the respective magnetic field configurations. Blue curves intersect at $\theta$ = 160° and $\phi$ = 65°. Red curves intersect at $\theta$ = 153° and $\phi$ = 53°. Notably, the intersection points for the red and blue curves do not coincide with each other in Figure 4.3

In Figure 4.3, certain segments of the red and blue curves overlap, indicating that some NV axes perceive identical magnetic field directions and magnitudes. Conversely, the non-overlapping portions suggest that other NV axes experience different magnetic field vectors. This demonstrates that NV centers are capable of detecting changes in both the direction and magnitude of the magnetic field.

### 4.2.2 ODMR signal with small angle differences

This section examines the system's ability to resolve small angular differences in magnetic field orientation by varying one angle while keeping the other constant. Two subcases are considered: (1) varying the polar angle $\theta$ while holding the azimuthal angle $\phi$ constant, and (2) varying $\phi$ while keeping $\theta$ fixed. Each subcase is evaluated through magnetic field reconstruction based on the corresponding ODMR signals.

In the first subcase, $\theta$ is varied slightly while $\phi$ is fixed at 165°. The red ODMR signal corresponds to $\theta$ = 68°, and the blue signal to $\theta$ = 70°. The computed results yield solution sets represented by red and blue curves in spherical coordinate space. At first glance, these curves appear to intersect at the same point. However, upon closer inspection of the small graph, the intersection points differ slightly, and the calculated angles are closely aligned with the actual input values. This indicates that the magnetic field calculation accurately resolves small variations of $\theta$ in Figure 4.4. In addition, if the curves do not intercept, we average the center area for defining interception.

In the second subcase, $\phi$ is varied while $\theta$ is fixed at 70°. The red ODMR signal corresponds to $\phi$ = 157°, and the blue signal to $\phi$ = 155°. Similar to the first case, the

resulting solution sets appear to overlap, but a magnified view of the graph reveals distinct intersection points. Again, the reconstructed angles closely match the original settings. These results in Figure 4.5 demonstrate that the magnetic field reconstruction method can effectively distinguish between similar ODMR spectra corresponding to nearby magnetic field orientations. The method is sensitive to subtle changes in both polar and azimuthal angles, highlighting its robustness and precision.

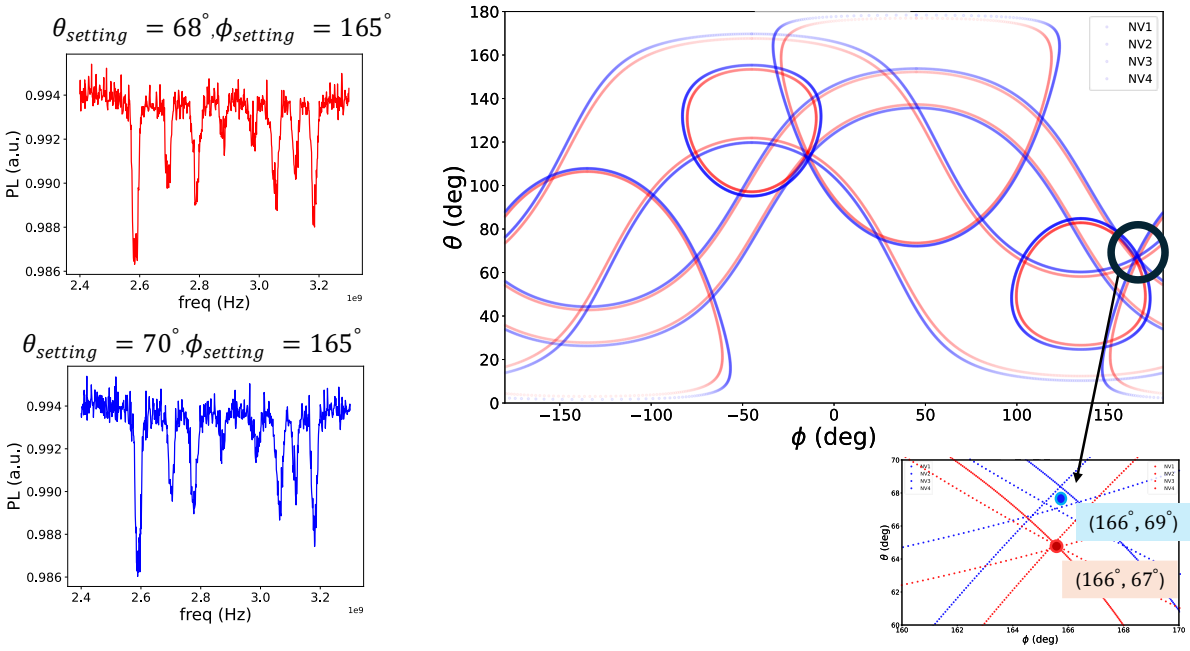


**Figure 4.4** the two ODMR signals with small difference acquired when $\theta$ and $\phi$ is set to 68°, 156° (red), and 70°, 165° (blue). The blue and red curves are the calculated result of NV axes. The calculated result present that the calculation distinguishes the small difference in the small figure when calculated $\theta$ and $\phi$ is 69°, 166° (red dot), and 67°, 166° (blue dot).

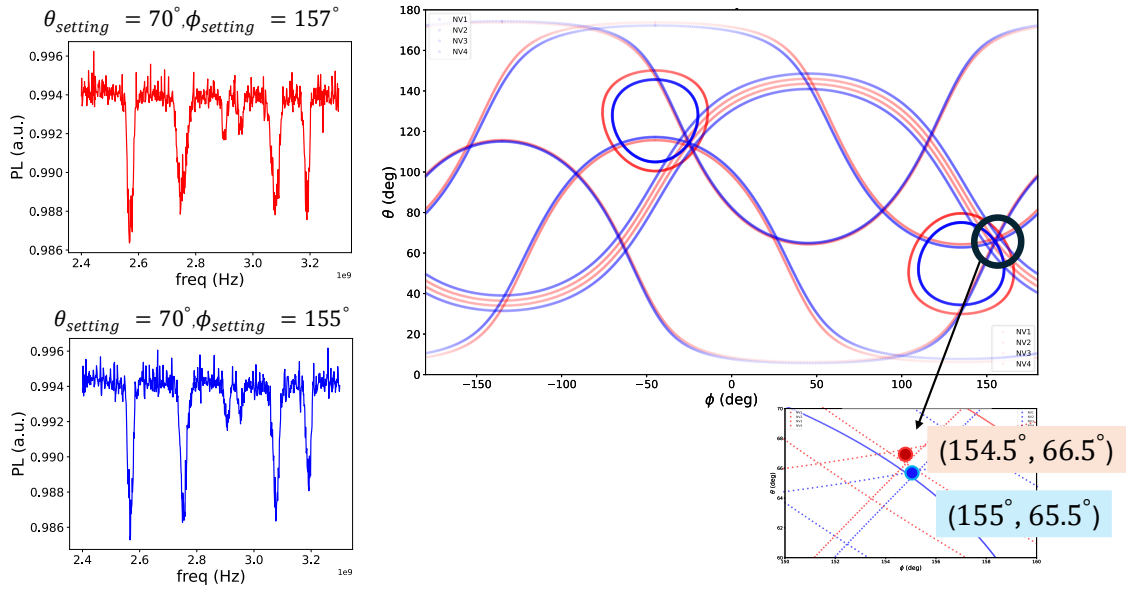


**Figure 4.5** the two ODMR signals with small differences acquired when $\theta$ and $\phi$ is set to 70°, 157° (red), and 70°, 155° (blue). The blue and red curves are the calculated results of NV axes that sense difference in from the blue and red ODMR signal respectively. The calculated result present that the calculation distinguishes the small difference in the small figure when calculated $\theta$ and $\phi$ is 66.5°, 154.5° (red dot), and 65.5°, 155° (blue dot).

## 4.3 NV center as a magnetic field scanner

Previously, we demonstrated vector magnetometry with ensemble NV center. IN this case, the NV center is going to be used as a sensor to image $\vec{B}$ from permanent magnet in the north pole direction in the new perspective.

Typically, when measuring the magnetic field at a specific location, a magnetic field sensor is placed directly at that position to detect both the field's magnitude and direction. In Figure 4.6, the black box with arrows indicating the magnetic field direction represents the magnetic field sensor, while the gray box denotes the magnet. When the sensor is positioned on the left side, it detects a magnetic field oriented in a southwest direction. As the sensor is moved toward the center of the region, the detected direction gradually shifts to the North Pole. At the system's center, the field direction points directly to the North Pole. Moving the sensor to the right-side results in a continued change in direction,

now pointing southeast direction. Notably, the magnetic field direction at the right side is approximately opposite to that on the left. This configuration is referred to as the **"scanning-NV perspective"**, wherein the NV center functions as a fixed sensor scanning the magnetic field.

In our experimental setup, however, the NV center cannot be moved due to physical constraints. To demonstrate vector magnetometry using NV centers under these conditions, the magnet itself is moved instead. This approach is termed the **"moving-magnet perspective"**. Figure 4.7 illustrates a comparison between these two perspectives: panels a), b), and c) show the moving-magnet perspective, while panels d), e), and f) depict the corresponding scanning-NV perspective. For example, in the moving-magnet configuration, when the magnet is placed at position A, the sensor detects a field pointing. In the corresponding scanning-NV view, this same field orientation appears reversed due to the frame of reference. When the magnet is positioned at the center (position B), the moving-magnet perspective detects a field pointing outward, while the scanning-NV perspective again shows an opposing direction. Similarly, at position C, the detected field direction in the moving-magnet setup is opposite to that at position A, while in the scanning-NV configuration, it remains consistent in its reversed relation.

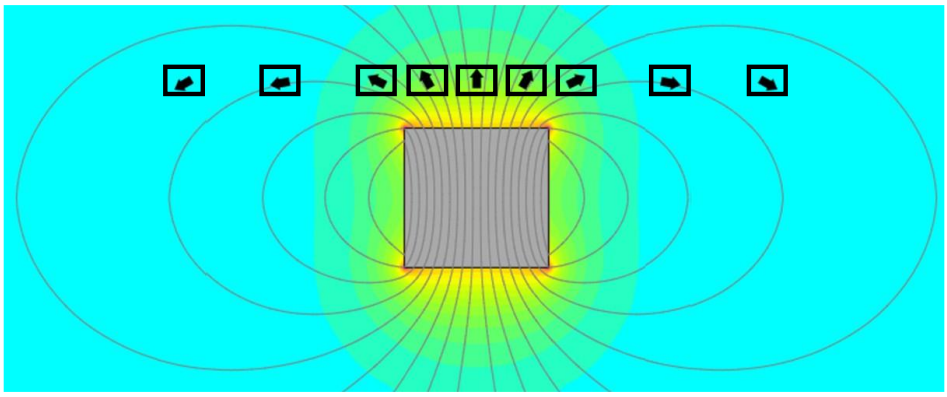

**Figure 4.6** The magnetic field in scanning-NV perspective is observed by sensor. When the magnetic field sensor is moved gradually from the left position to the center position, the magnetic field direction is changed from the left direction to pointing out of the magnet. Moving sensor from the center magnet to the left positions is changed direction from pointing out to right direction.

Consequently, all experimental results are reported in the scanning-NV perspective, with interpretations flipped from the moving-magnet reference frame. Furthermore, the experiment is designed to observe the magnetic field near the north pole of the magnet, where the field diverges outward from the magnet's center, and the magnitude decreases with increasing distance from the center.

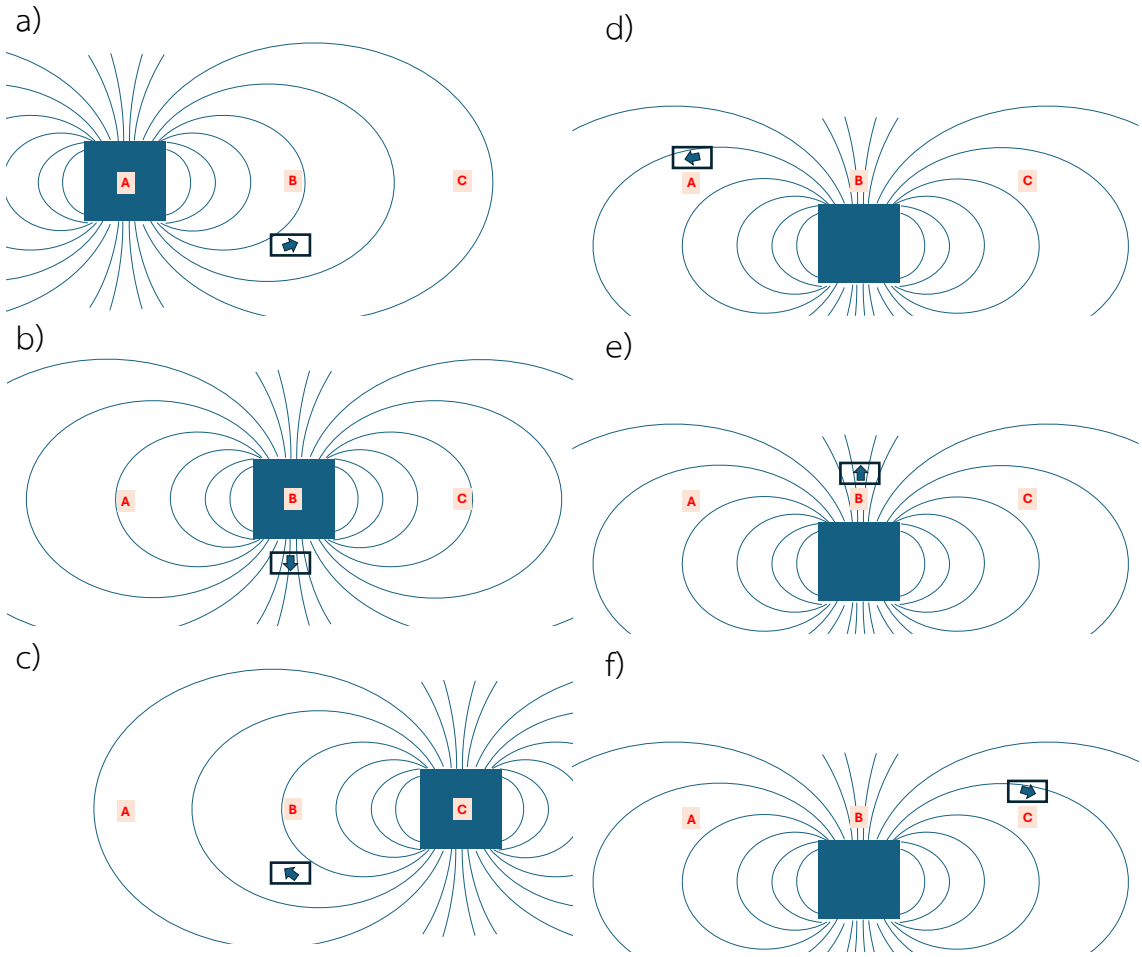


**Figure 4.7** The picture a), b), c) represent magnet is moved at the different position and NV center sense different magnetic field direction as a position in moving-magnet perspective. The picture d), e), f) pictures represent the corresponding scanning-NV perspective of a), b), c) respectively. When NV is a small box with arrow indicating the magnetic field direction, and magnet is blue box.

## 4.4 Setup for magnetometry

Due to the constraints of the experimental setup, the magnet is moved instead of the sensor. To facilitate this, the dial component of the setup was removed, and a flat plate was positioned approximately 1.7 cm above the NV center. A sheet of graph paper was affixed to the plate to define a coordinate system for the magnet's movement in the x and y directions, as illustrated in Figure 4.8. During the experiment, the ODMR signal was measured as a function of the magnet's position across 5 x 5 cm detection area (see Figure 4.9). The collected data were organized into a two-dimensional array corresponding to spatial positions. Each data point was then processed using a magnetic field reconstruction algorithm to determine the local magnetic field magnitude and orientation. Finally, the results of the calculation were used to extract the magnetic field components in the x, y, and z directions at each measurement position.

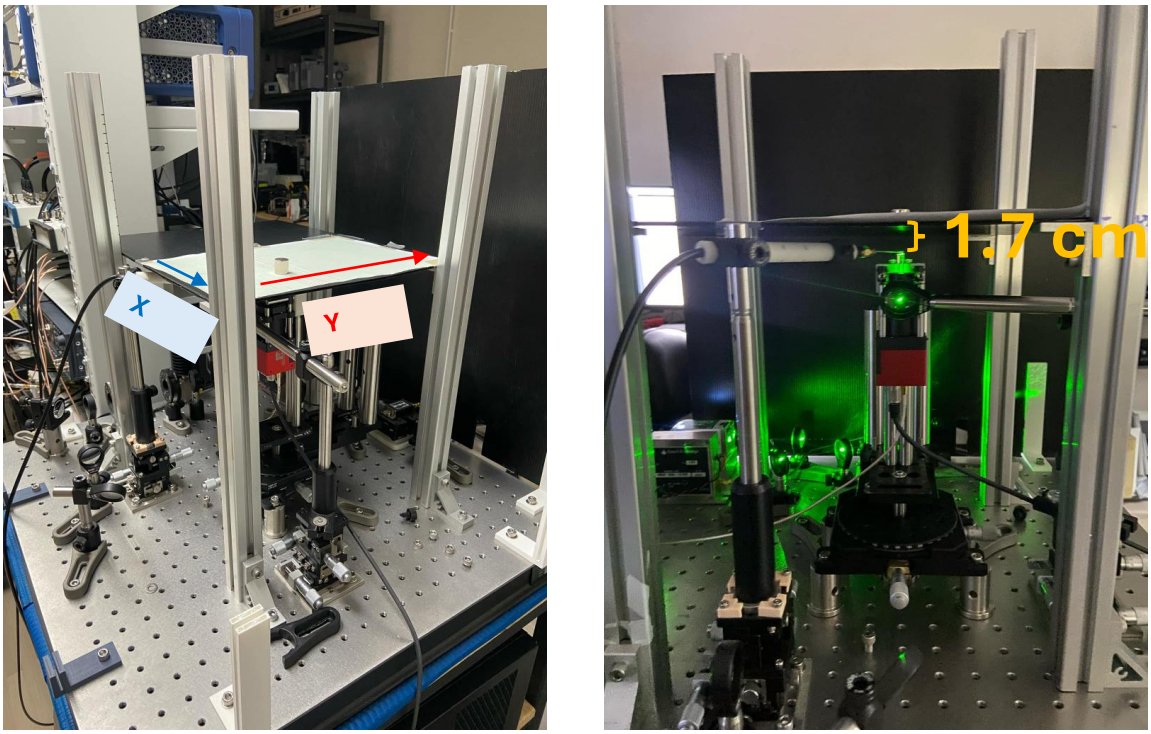


**Figure 4.8** The new setup without magnet on dial has a plate for moving magnet plane with magnet on the top of plate. The distance between magnet and NV center on the top of lightguide is 1.7 cm.

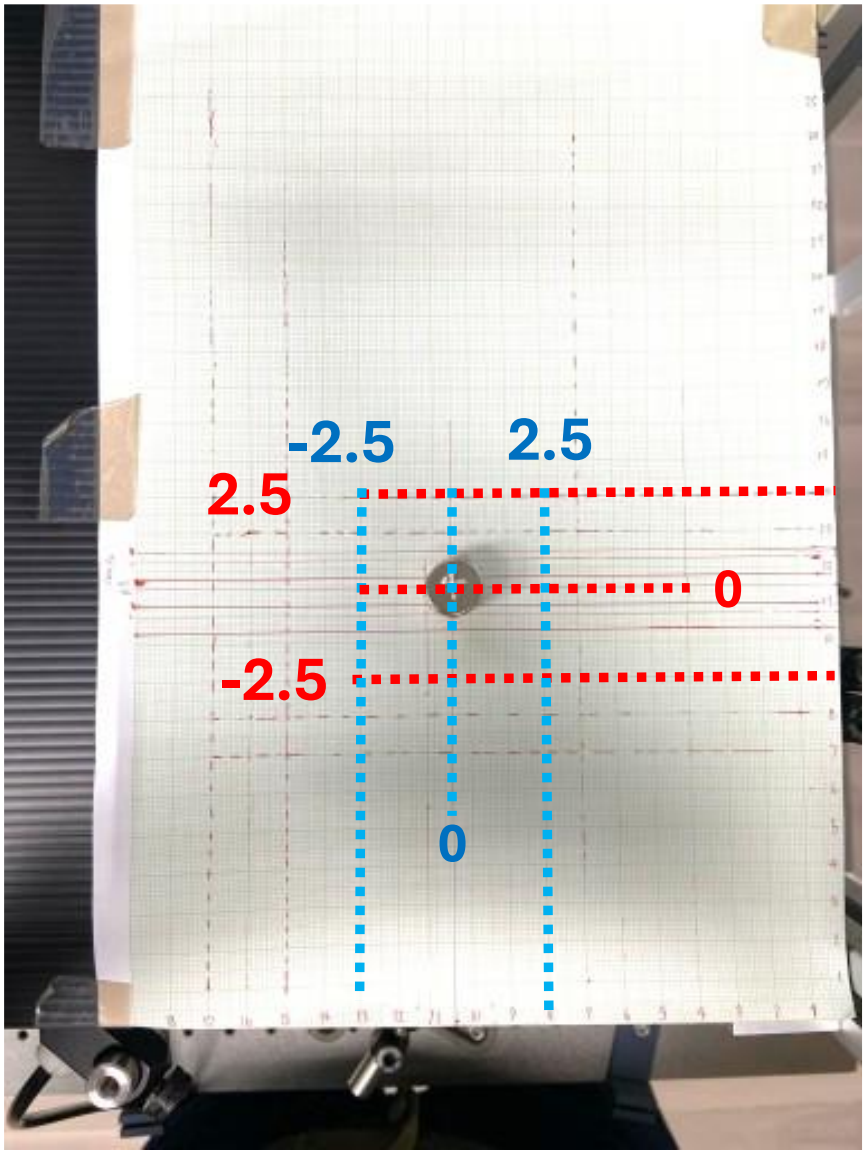


**Figure 4.9** The plate is attached by graph paper. The graph shows detection area for experiment with setting the center of the system at 0 and border from 2.5 to -2.5 in x and y direction.

## 4.5 Magnetic field strength above the NV center at 1.7 cm

In vector magnetometry, the results—presented from the scanning-NV perspective—include the total magnetic field magnitude $B_{total}$, as well as the individual

magnetic field components along the z-axis ($B_z$), x-axis ($B_x$), and y-axis ($B_y$), all plotted on the same spatial scale in the xy plane in Figure 4.10.

The $B_{total}$ illustrates the spatial distribution of field strength across the xy plane. At the center of the detection area, the magnitude reaches its maximum value due to the proximity of the magnet to the NV center. As the magnet is moved away from the center, the field strength decreases gradually, with more significant attenuation observed at the outer edges of the detection region.

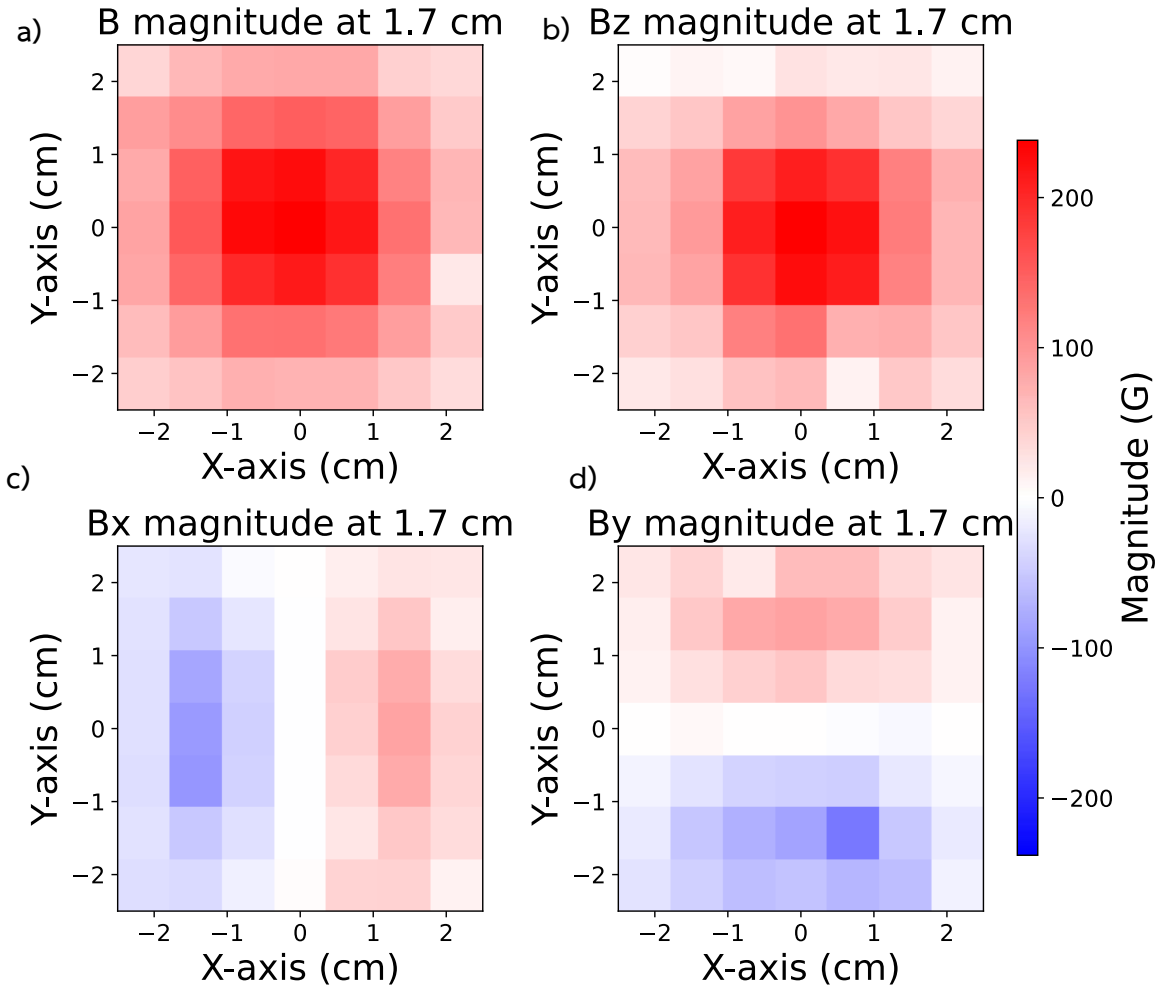


**Figure 4.10** In this figure represent magnetic field gradient above the NV center at 1.7 cm. Each picture present magnetic field in cartesian coordinate. a) $B_{total}$ b) $B_z$, c) $B_y$, d) $B_x$.

The individual field components—$B_z$, $B_y$ and $B_x$—provide directional insight into the magnetic field vector. At the central position, the field is predominantly oriented along the z-axis ($B_z$), indicating that the field lines point outward from the magnet's surface. Consequently, $B_x$ and $B_y$ are approximately zero at the center. As the magnet is displaced from the center, the field direction shifts, resulting in non-zero x and y components. This change arises because the magnetic field is no longer perpendicular to the NV axis, allowing the NV center to detect components in all spatial directions.

Notably, along the x = 0 and y = 0 lines, the $B_x$ and $B_y$ components are zero, respectively, due to the symmetry of the magnetic field distribution. This behavior is consistent with theoretical expectations.

These results confirm that NV centers can effectively map the spatial variation of the magnetic field vector near the magnetic north pole, demonstrating the feasibility of high-resolution vector magnetometry.

## 4.6 Magnetic field direction above the NV center at 1.7 cm

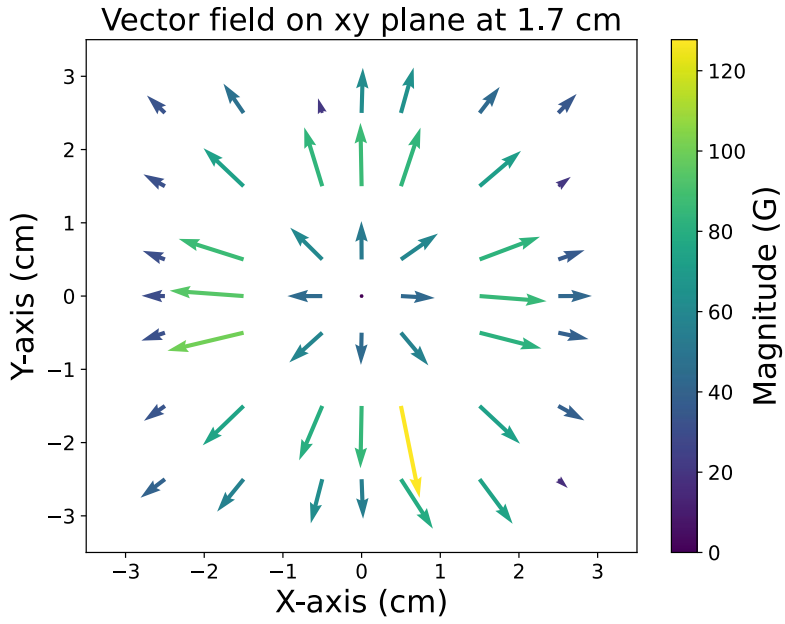


**Figure 4.11** Vector field present the distribution of magnetic field in x and y direction in xy plane at 1.7 cm.

Typically, the magnetic field near the north pole of a magnet radiates outward from the magnet's surface into the surrounding space. In this context, the vector field representation captures the direction and distribution of the magnetic field within the xy plane in figure 4.11. At the center of the detection area, the magnetic field is oriented primarily along the z-axis, resulting in no visible in-plane xy components. However, immediately surrounding the center, the magnetic field vectors point outward, and the field magnitude is relatively high due to the proximity of the magnet to the NV center.

As the magnet is positioned further from the NV center, the field magnitude decreases gradually, but the vector direction continues to point outward, maintaining the radial pattern characteristic of a dipolar field.

This observed vector field behavior is consistent with the magnetic field gradient analysis discussed in Section 4.5, further validating the experimental results.

## 4.7 Magnetic field at 3 different heights

In this experiment, the NV center is used to demonstrate vector magnetometry at varying vertical distances from the magnet. The magnetic field at different heights interacts with the NV center differently, influencing the detected ODMR signal. Measurements were conducted at heights of 1.2 cm, 1.7 cm, and 2.2 cm above the NV center. At each height, the ODMR signal was recorded at multiple positions across the sensing area and used to reconstruct the spatial magnetic field vector.

At a height of 1.2 cm, ODMR signals near the central region could not be used in the analysis because the Zeeman splittings exceeded the frequency sweep range. $B_z$, $B_y$ and $B_x$

Figure 4.12 presents the calculated magnetic field gradients—total magnitude as well as the $B_x$, $B_y$, and $B_z$—across the three height levels. As the magnet approaches the NV center, the magnetic field gradient increases. This is particularly evident at the system’s center, where the field strength is highest, and the gradient contrast is more important The spatial extent of the strong magnetic field also becomes more localized around the center.

Similarly, both $B_x$ and $B_y$ increase significantly at lower heights, as shown by the higher contrast in their respective gradient maps. The behavior of $B_z$, however, is more complex. At positions far from the center, $B_z$ points outward from the magnet and gradually transforms into $B_x$ and $B_y$ components as the field becomes less aligned with the z-axis. Near the NV center, $B_z$ increases only around the central region, while decreasing in surrounding areas due to a shift in the magnetic field direction.

This shift represents a transition from a field pointing outward along the z-axis to one becoming more perpendicular to the NV axis. If the measurement area were extended, the z-component of the magnetic field would eventually flip direction and point downward—indicating a transition from the magnetic north pole to the south pole. These results are consistent with the expected field behavior near the magnetic poles in the xy plane.

In a vector field representation in Figure 4.13, the magnetic field near the north pole typically radiates outward from the center. The figure illustrates the magnetic field vectors at three different vertical distances in the xy plane. When the magnet is positioned farther from the NV center, the field vectors are weaker and more localized, extending only a short distance from the center. In contrast, when the magnet is positioned closer to the NV center, the magnetic field becomes stronger and its influence extends farther across the detection area, resulting in a more widely distributed vector field.

In the xz and yz planes, the vector field in Figure 4.14 is visualized along the central vertical line for three different height levels. The results show that the magnetic field direction radiates outward from the magnet, consistent with dipolar field behavior. As the NV center is positioned closer to the magnet, the field strength increases noticeably.

At a height of 1.2 cm, the magnetic field component in the z-direction near the edge of the detection area approaches zero. If measurements were extended beyond this region, the z-component of the magnetic field would reverse direction, indicating a transition from the magnetic north pole to the south pole. This polarity flip is clearly observed in both the xz and yz plane vector field plots.

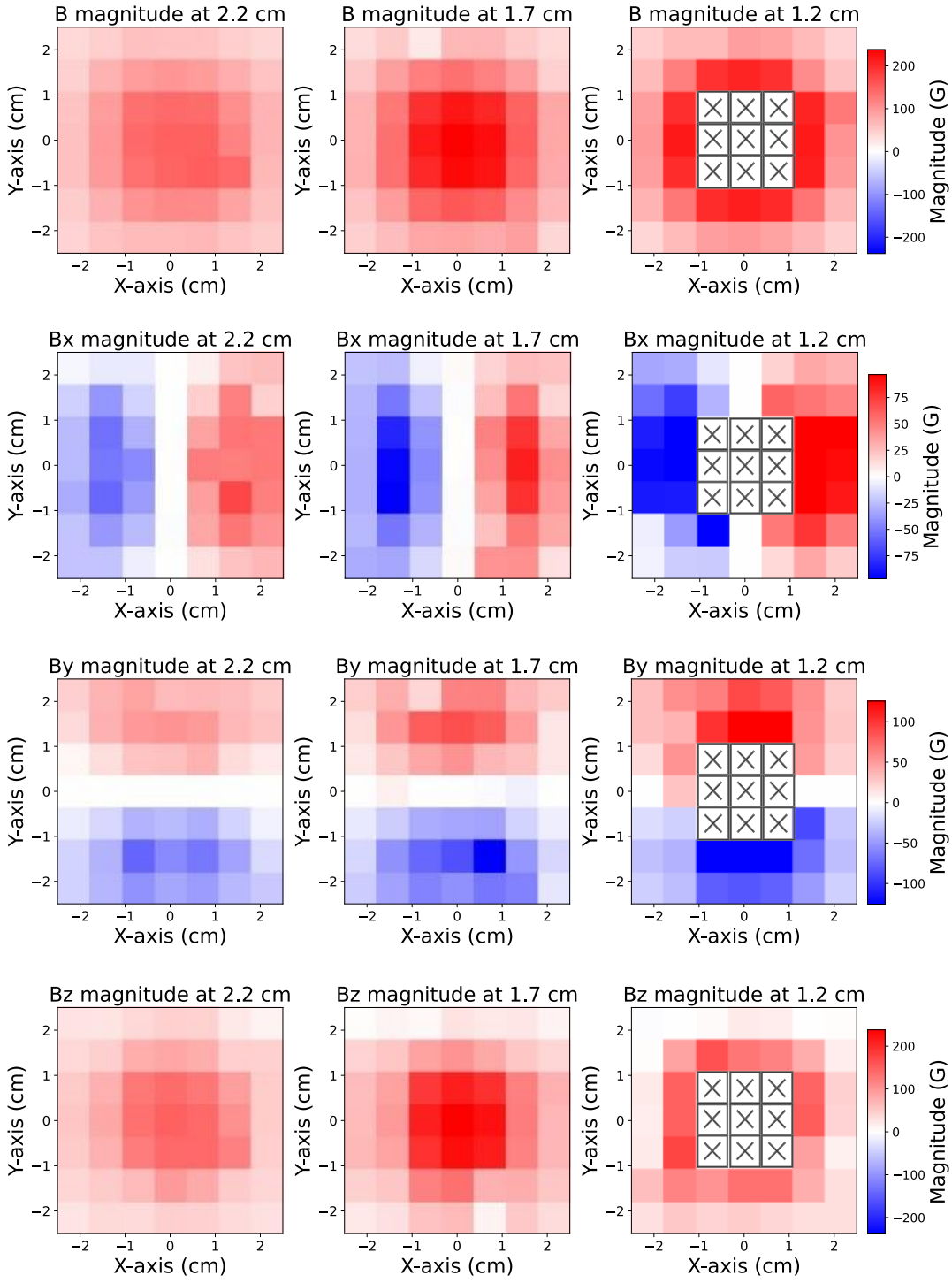


**Figure 4.12** The graph represents magnetic field gradient at $B_{total}$, $B_x$, $B_y$ and $B_z$ at different height above the NV center. At 1.2 cm, the cross present unmeasured area.

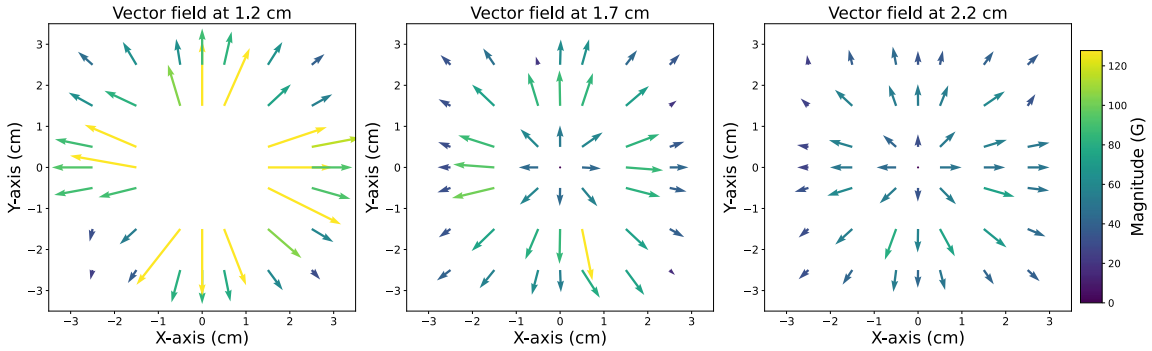


**Figure 4.13** The graph represents vector field of magnetic field at the different heights above the NV center in xy plane.

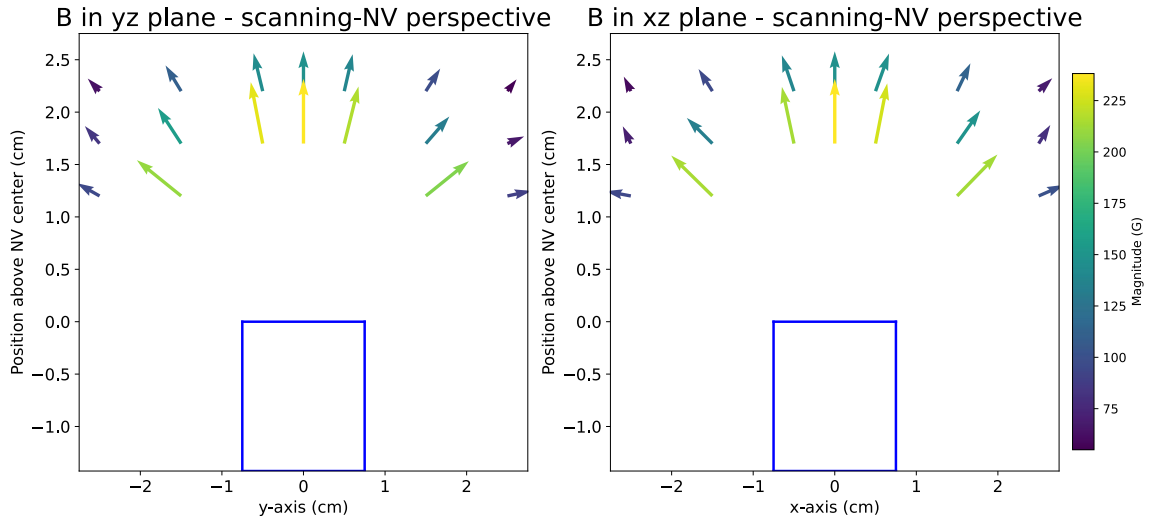


**Figure 4.14** The graph represents magnetic field in yz and xz plane at the central line of y and x axis.